ISSN (Print) 1226-1750
ISSN (Online) 2233-6656
Journal of Magnetics 27(2), 217-222 (2022) https://doi.org/10.4283/JMAG.2022.27.2.217

Comparison of a Zero-filling Interpolation with a Real Matrix Size at 1.5 Tesla Based on Spin-echo Weighted Imaging with Various Spatial Resolutions: An ACR Phantom Study

Ji Sung Jang[1], Ho Beom Lee[1], Seok Hwan Yoon[2], Min Cheol Jeon[3], and Seong Ho Kim[3]*

[1]Department of Radiology, Asan Medical Center, Seoul 05505, Korea
[2]Department of Nuclear Medicine, Seoul National University Hospital, Seoul 03080, Korea
[3]Department of Radiological Technology, Daejeon Health Institute of Technology, Daejeon 34504, Korea

(Received 13 April 2022, Received in final form 8 June 2022, Accepted 8 June 2022)

This study aimed to assess the effect of zero-filling interpolation (ZIP) and various spatial resolutions on quality assurance (QA). Two important variables for the assessments of magnetic resonance image quality were included with recommended acceptance criteria: high-contrast spatial resolution and low-contrast object detectability with reference limits. All acquired data were divided into two groups: group A (without ZIP) and group B (with ZIP). The spatial resolutions of both images of T1-weighted and T2-weighted imaging in both directions fulfilled the American College of Radiology (ACR) criterion in group B. The observed high-contrast spatial resolution values were significantly different between the two groups up to a matrix size of 320 × 320 ($p < 0.05$). On the other hand, with a matrix size ≥ 384 × 384, no significant differences between the two groups were observed in terms of high-contrast spatial resolution ($p > 0.05$). For low-contrast object detectability, the total number of measured spokes in all groups fulfilled the ACR criterion. However, the low-contrast object detectability values without ZIP tended to decrease as the matrix size decreased. The use of ZIP can improve high-contrast spatial resolution and low-contrast object detectability while reducing image blurriness.

Keywords : zero filling interpolation, ACR phantom, quality assurance, spatial resolution, matrix size

1. Introduction

Although magnetic resonance (MR) imaging is widely known as outstanding with respect to both soft-tissue contrast ratio and resolutions compared to other medical imaging techniques, the MR image sampling process in k-space increases the image acquisition time owing to its unique physiological and hardware characteristics. Additionally, increased sampling time not only cause patients discomfort, but can also potentially result in motion artifacts [1, 2].

In MR imaging applications, the processing of MR data is typically performed using a Fast Fourier-Transform (FFT) for imaging. These mathematical algorithm processes typically require that the input raw data be placed in a matrix with squared dimensions, such as 128 ×128, 256 × 256, or 512 × 512. However, if the acquired k-space data does not fulfill this matrix, inserting of zero value into matrix for missing data is a common process. In summary, this process is known as zero-filling interpolation (ZIP), which increases the matrix size of new data by replacing unmeasured data point with zero value before the FFT is applied to the MR data. As a result, pixel sizes will be smaller than the image's actual matrix size [3-6].

Doubling of the number of data points in k-space initially using ZIP goes beyond simple interpolation and actually adds fresh information rather than creating new information. Because the general FFT does not extract all of the information available in a free induction decay (FID), doubling the number of data points makes the FFT more efficient to extract all true data needed for MR imaging [7]. However, several studies have shown that ZIP and resampling can sometimes result in artifacts that noticeably degrade the sharpness of enlarged image [8-10].

Theoretically, high-resolution acquisition is a way to address this problem, but it is difficult to apply clinically because factors affecting image acquisition, such as a longer scan time and lower signal-to-noise ratio (SNR), should be considered. To the best of our knowledge, image-comparing studies of quality assurance (QA) are rare, with no studies focusing on QA comparisons of different spatial resolutions in combination with ZIP [11-13]. Therefore, this study aimed

*Corresponding author: Tel: +82-42-670-9174
Fax: +82-42-670-9570, e-mail: pooh79@hit.ac.kr

to assess the effect of ZIP and various spatial resolutions on QA.

2. Materials and Methods

2.1. Phantom study

An MR phantom for head imaging, approved by the American College of Radiology (ACR) (JM, Specialty Parts, J9467, San Diego, CA, USA), was used for the phantom measurements and analysis in our study. The internal dimensions of the ACR cylindrical phantom were 148 mm in length × 190 mm in diameter. The phantom was consisted of a solution of nickel chloride and sodium chloride (10 mM NiCl2 and 75 mM NaCl) and was carefully positioned so that the center of the phantom was aligned with the iso-center of the scanner by indicator laser light according to its nose and chin landmarks [14]. Room temperature (21.0 °C) was maintained to avoid temperature dependence of the quantitative measurements of image data. All acquired data were divided into two groups according to whether the ZIP technique was applied: group A (without ZIP) and group B (with ZIP).

2.2. MR equipment and scan parameters

All data were performed using 1.5 T scanners (Avanto; Siemens Healthcare, Erlangen, Germany) with a 45 mT/s maximum amplitude, a slew rate of 200 T/m/s, and a 12-channel head coil. The site sequence series based on the scan parameters the site normally used in its clinical protocols were used to acquire spine echo sequence T1-weighted imaging (T1WI) and turbo spin echo sequence T2-weighted imaging (T2WI) axial orientation according to the phantom test guidance for the ACR MR imaging accreditation program. The uniformity correction scan option was used to improve the image intensity uniformity. The scan parameters for both MR sequence modes were as follows: field of view, 250 × 250 mm; slice thickness, 5 mm; slice gap, 5 mm; receiver bandwidth, 110 Hz/pixel; flip angle, 90°; number of slices, 11. A detailed description of the parameters is presented in Table 1. Various matrix sizes were adjusted in five steps (256 × 256, 320 × 320, 384 × 384, 448 × 448, and 512 × 512) to evaluate the usefulness of the ZIP technique. Image acquisition time according to matrix size and MR sequence is presented in Table 2.

2.3. Image analysis

For QA of the study method, ACR phantom images were evaluated and obtained with and without the ZIP technique. To analyze the quality of the acquired images, a total of 11 slices images were acquired using ACR phantom, and then ACR MR imaging quality control measurement consisting of two quantitative analysis was performed on ten sets of scans obtained under the same setup condition for each matrix size both with and without ZIP using open-source Matlab code (R2016b; Mathworks, Natick, MA, USA) available from http://jidisun.wix.com/osaqa-project [15].

Two quantitative tests were conducted as follows: high-contrast spatial resolution and low-contrast object detectability evaluations. The ZIP technique was used to evaluate the ability to distinguish objects by contrast noise ratio (CNR). For these reasons, we excluded other quantitative ACR tests. The images were evaluated according to the ACR instructions by a single observer, and the measured results were compared to the ACR criterion. The measurement was performed twice for each condition. The high-contrast spatial resolution in a slice-1 image was visually evaluated based on the distinguishability of hole-array pairs with hole diameters of 0.9 mm, 1.0 mm, and 1.1 mm (Fig. 1). Low-contrast object detectability was visually evaluated by counting the number of visible objects in four images from slices 8 to 11 with gradually decreasing contrast and object size (Fig. 2).

2.4. Statistical analysis

The high-contrast spatial resolution and low-contrast

Table 1. Detailed summary of the common image acquisition parameters in all groups.

	FOV (cm)	TR (ms)	TE (ms)	Slice thickness / gap (mm)	NEX	BW (Hz)	FA
T1WI	25	500	20	5 / 5	1	110	90
T2WI	25	3000	80	5 / 5	1	110	90

T1WI, T-weighted imaging; T2WI, T2-weighted imaging; FOV, field of view; TR, repetition time; TE, echo time; NEX, number of excitations; BW, bandwidth; flip angle, FA

Table 2. Image acquisition time according to matrix size and MR pulse sequence.

Sequence	Matrix size				
	256	320	384	448	512
T1WI	2 min 12 sec	2 min 44 sec	3 min 16 sec	3 min 48 sec	4 min 20 sec
T2WI	4 min 06 sec	5 min 06 sec	6 min 06 sec	7 min 06 sec	8 min 06 sec

T1WI, T- weighted imaging; T2WI, T2-weighted imaging; MR, magnetic resonance

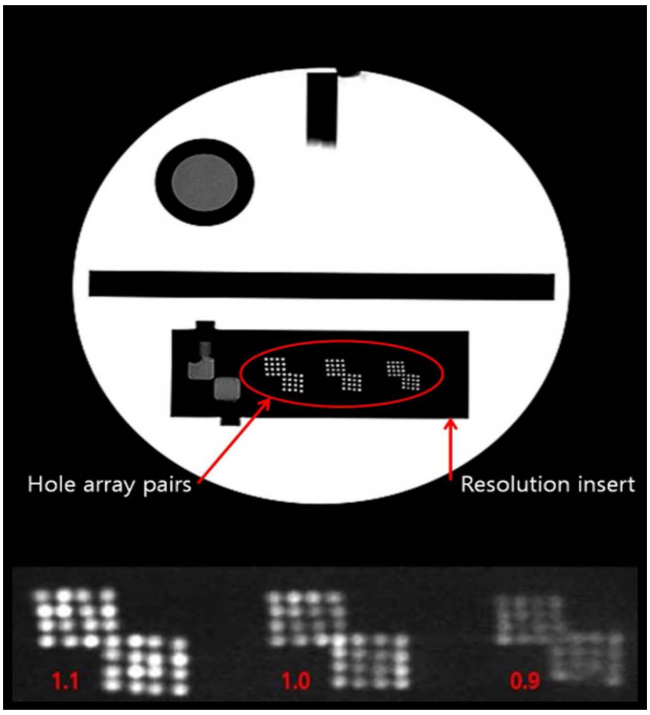

Fig. 1. (Color online) Magnified images (slice 1) used for visually assessing high-contrast spatial resolution that based on the distinguishability of hole-array pairs with hole diameters of 0.9 mm, 1.0 mm, and 1.1 mm (from left to the right).

object detectability measurements obtained with and without ZIP using various matrix sizes in association with both MR sequence modes were compared using analysis of variance (ANOVA). When statistically significant differences were indicated, post-hoc tests were performed using the Tukey-Kramer method. Statistical analyses were performed using SPSS Statistics for Windows version 21.0 (IBM Corp., Armonk, NY, USA). For all statistical analyses, a two-sided probability level of $p < 0.05$ was considered statistically significant.

3. Results

The measured resolution values for high-contrast spatial resolution testing in association with both MR sequence modes are presented in Table 3. The spatial resolution values of T1WI and T2WI in both directions fulfilled the ACR criterion of 1.0 mm in all applied ZIP groups regardless of matrix sizes. The high-contrast spatial resolution values tended to decrease as matrix size decreased, and the high-contrast spatial resolution exhibited particularly significant decreases at matrix sizes of 256 × 256 and 320 × 320 without ZIP. At matrix sizes of 256 × 256 and 320 × 320 in both MR sequence modes, there were significant intergroup differences in spatial resolution values in both directions ($p < 0.05$). In particular, spatial resolution values for the 256 × 256 matrix size without ZIP were 1.1 mm with both MR sequence modes (failing to fulfill the ACR criterion). On the other hand, in the case of a matrix size ≥ 384 × 384, all spatial resolution values were 0.9 mm and fulfilled the ACR criterion, regardless of whether ZIP was used, in association with both MR sequence modes. Additionally, no statistically

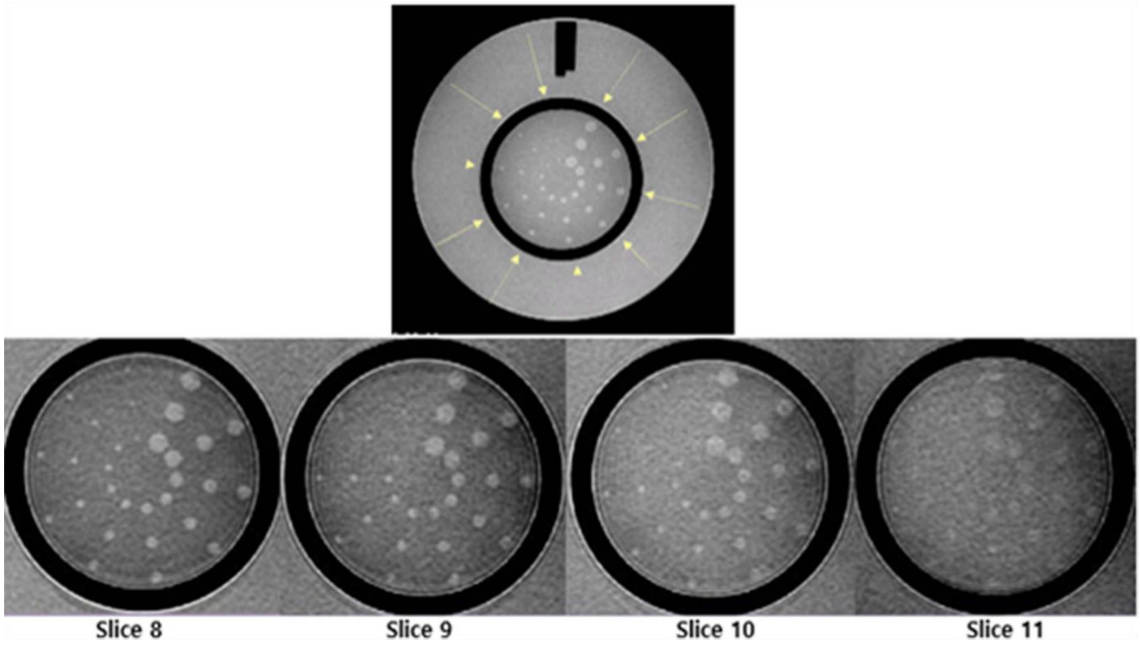

Fig. 2. (Color online) Magnified and cropped images used to visually evaluate the low-contrast object detectability by counting the number of objects visible in four images from slices 8 to 11 with gradually decreasing contrast and object size. Each spoke is made up of 3 disks, and there are 10 spokes om each circle.

Table 3. Results of high-contrast spatial resolution obtained with and without ZIP for various matrix sizes in association with both MR pulse sequences.

Test	Sequence	Application	Direction	Matrix size				
				256	320	384	448	512
High-contrast spatial resolution	T1WI	Without ZIP	UL	1.1*‡	1.0†	0.9	0.9	0.9
			LR	1.1*‡	1.0†	0.9	0.9	0.9
		With ZIP	UL	1.0*†	0.9	0.9	0.9	0.9
			LR	1.0*†	0.9	0.9	0.9	0.9
	T2WI	Without ZIP	UL	1.1*‡	1.0†	0.9	0.9	0.9
			LR	1.1*‡	1.0†	0.9	0.9	0.9
		With ZIP	UL	1.0*†	0.9	0.9	0.9	0.9
			LR	1.0*†	0.9	0.9	0.9	0.9

Notes: When statistically significant differences were indicated using Tukey-Kramer post-hoc analysis, the symbols *, †, and ‡ were used to indicate p-values ($p < 0.05$) between 1.1 and 1.0 (*), between 1.0 and 0.9 (†), and between 1.1 and 0.9 (‡). UL, upper left; LR, lower right; T1WI, T-weighted imaging; T2WI, T2-weighted imaging; ZIP, zero-filling interpolation; MR, magnetic resonance

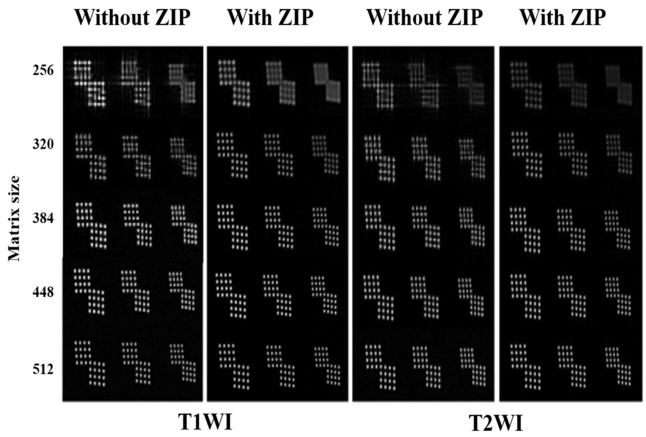

Fig. 3. The cropped ACR phantom images (slice 1) of the high-contrast spatial resolution obtained with and without ZIP according to different matrix sizes (256 × 256 through 512 × 512) in association with both MR sequence modes.

significant intergroup differences were found in terms of high-contrast spatial resolution ($p > 0.05$). The measured high-contrast spatial resolutions without ZIP were generally low compared with those with ZIP (Table 3). Fig. 3 shows the representative images of high-contrast spatial resolution obtained with and without ZIP according to various matrix sizes in association with both MR sequence modes. Notably, blurring was more noticeable in images of all matrix sizes without ZIP than when ZIP was applied, even if measured spatial resolution values fulfilled the ACR criterion.

For low-contrast object detectability, the total number of measured spokes in the two groups was ≥ 37, fulfilling the ACR criterion of greater than nine spokes for 1.5 T. Table 4 shows the low-contrast object detectability values of images obtained with and without ZIP for various matrix sizes with both MR sequence modes. In general, the low-contrast object detectability values without ZIP tended to decrease as the matrix size decreased. The observed low-contrast object detectability values were significantly different between the two groups up to a matrix size of 320 × 320 ($p < 0.05$). On the other hand, in the case of matrix sizes ≥ 384 × 384, no statistically significant intergroup differences were found in either MR sequence mode in terms of low-contrast object detectability ($p > 0.05$) (Table 4). Representative images acquired from both groups are shown in Fig 4.

Table 4. Results of low-contrast object detectability obtained with and without ZIP for various matrix sizes in association with both MR pulse sequences.

Test	Sequence	Application	Index	Matrix size				
				256	320	384	448	512
Low-contrast object detectability	T1WI	Without ZIP	Total	37*	38‡	40	40	40
		With ZIP	spoke	40	40	40	40	40
	T2WI	Without ZIP	Total	38‡	38‡	40	40	40
		With ZIP	spoke	40	40	40	40	40

Notes: When statistically significant differences were indicated using Tukey-Kramer post-hoc analysis, the symbols * and ‡ were used to indicate p-values ($p < 0.05$) between 37 and 40 (*), and between 38 and 40 (‡). T1WI, T1-weighted imaging; T2WI, T2-weighted imaging; ZIP, zero-filling interpolation

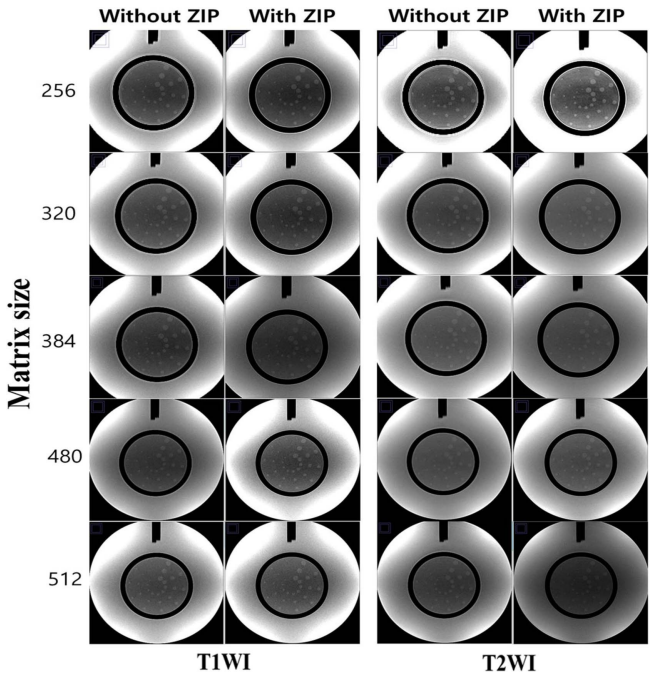

Fig. 4. ACR phantom images (slice 11) of the low-contrast object detectability obtained with and without ZIP according to different matrix sizes (256 × 256 through 512 × 512) in association with both MR sequence modes. All images (spokes ≥ 37) fulfilled the ACR criterion of greater than nine spokes for 1.5 T.

4. Discussion

Our study demonstrated the effectiveness of ZIP for improving high-contrast spatial resolution and low-contrast object detectability values using the ACR QA test. Previous studies have shown that ZIP efficiently increases spatial resolution by allowing spatial corner data while reducing partial volume artifact [3, 4]. On the other hand, some studies have shown that ZIP produces artifacts in resampling images [9, 10]. Additionally, ZIP not only affects high-frequency components but also produces blurred images. For this reason, the application of ZIP is controversial to some extent, and it should be carefully considered depending on clinical examination findings or MR pulse sequence mode. We demonstrated that the use of ZIP provides high-contrast spatial resolution and low-contrast object detectability comparable to high resolution.

We found that most values in the two evaluated categories fulfilled the ACR QA criteria, whether or not ZIP was applied. However, some comparisons have shown that those values are statistically different depending on whether ZIP was applied to all MR pulse sequences with matrix sizes $\leq 320 \times 320$. In addition, image blurring was significantly improved in high contrast spatial resolution by using ZIP. These observations can be explained by the fact that acquiring more data in the periphery of k-spaces associated with high spatial frequencies preserve sharp edges and image details and is less prone to blurring and Gibbs artifacts [16, 17]. If ZIP is used, and the corner data are not apodized, acquiring corner data improves the spatial resolution. The extent of image quality improvement was determined to vary according to the spatial resolution. Increasing the matrix size is one way to improve spatial resolution. However, this results in a low SNR and prolonged image acquisition time, which may cause artifacts related to patient motion. To address this limitation, increased matrix size with ZIP should be considered in comparison with increased matrix size without ZIP. A lower SNR caused by an increase in matrix size can be compensated for by using ZIP. Our results demonstrated that ZIP could maintain and improve image quality at relatively small matrix sizes. This means that ZIP can more effectively improve images of relatively low spatial resolution without increasing image acquisition time.

When using the ACR phantom for quantitative and qualitative image quality analysis, it is important to present definitive and objective criteria. However, manual assessment methods appear to be time-consuming, complicated, and inefficient for assessing image quality, tending to be highly dependent on the observer or the size of the monitor being used. Previous studies have presented automatic analysis methods for reducing QA processing times while improving the repeatability and objectivity of measured values [15, 18]. That is why we also used automatic image quality assessments available through open-source code, a measurement criterion that was relatively easy to perform and that minimized inter-observer variability in the measured values.

This study had several limitations. First, we used only the ACR phantom, which is mainly designed for QA and does not represent different organs, tissues, or specific target lesions. Second, this study only used a 1.5-T MR scanner from one vendor. Due to this constraint, the study findings must be interpreted with caution. Further research is warranted to demonstrate the effects of a variety of software applications and magnetic field strengths on image quality. Nevertheless, this study is meaningful because it was the first to analyze various matrix sizes to evaluate the study question and the first to evaluate image quality in terms of ZIP implementation and spatial resolution.

5. Conclusion

ZIP can improve high-contrast spatial resolution and low-contrast object detectability while fulfilling the ACR criteria and reducing image blurriness.

References

[1] M. Ran, W. Xia, Y. Huang, Z. Lu, P. Bao, *et al*., IEEE Transactions on Radiation and Plasma Medical Sciences **5**, 120 (2020).

[2] S. H. Ali, M. E. Modic, S. Y. Mahmoud, and S. E. Jones,

AJR Am. J. Roentgenol. **200**, 630 (2013).
[3] M. A. Bernstein, S. B. Fain, and S. J. Riederer, J. Magn. Reson Imaging **14**, 270 (2001).
[4] A. Ebel, W. Dreher, and D. Leibfritz, J. Magn. Reson. **182**, 330 (2006).
[5] J. C. Lindon and A. G. Ferrige, Progress in Nuclear Magnetic Resonance Spectroscopy **14**, 27 (1980).
[6] X. Zhu, B. Tomanek, and J. Sharp, Concepts in Magnetic Resonance Part A **42**, 32 (2013).
[7] E. Bartholdi and R. R. Ernst, J. Magn. Reson. **11**, 9 (1973).
[8] I. Aganj, B. T. Yeo, M. R. Sabuncu, and B. Fischl, IEEE. Trans. Image. Process **22**, 816 (2013).
[9] J. Parker, R. V. Kenyon, and D. E. Troxel, IEEE. Trans. Med. Imag. **2**, 31 (1983).
[10] S. K. Park and R. A. Schowengerdt, Appl. Opt. **21**, 3142 (1982).
[11] R. Lin, R. Wu, Z. Xiao, G. Liu, K. Kong, and Z. Lang, Rivista di Neuroradiologia. **18**, 169 (2005).
[12] Y. P. Du, D. L. Parker, W. L. Davis, and G. Cao, J Magn. Reson. Imaging **4**, 733 (1994).
[13] D. L. Parker, Y. P. Du, and Davis, Magn. Reson. Med. **33**, 156 (1995).
[14] H. B. Lee, J. S. Jang, K. B. Lee, and S. M. Kim, J. Appl. Clin. Med. Phys. **22**, 110 (2021).
[15] J. Sun, M. Barnes, M. J. Dowling, F. Menk, P. Stanwell, and P. B. Greer, Australas. Phys. Eng. Sci. Med. **38**, 39 (2015).
[16] R. Mezrich, Radiology. **195**, 297 (1995).
[17] T. A. Gallagher, A. J. Nemeth, and L. Hacein-Bey, AJR Am. J. Roentgenol. **190**, 1396 (2008).
[18] A. C. Epistatou, I. A. Tsalafoutas, and K. K. Delibasis, Journal of Imaging **6**, 111 (2020).